Reversibility between Glass and Melting Transitions of Poly(oxyethylene)

Wulin Qiu,[†,‡] Marek Pyda,[†,‡] Elisabieta Nowak-Pyda,[†] Anton Habenschuss,[‡] and Bernhard Wunderlich*[,†,‡]

Department of Chemistry, The University of Tennessee, Knoxville, Tennessee 37996-1600, and Chemical Sciences Division, Oak Ridge National Lab., Oak Ridge, Tennessee 37831-6197

Received April 22, 2005; Revised Manuscript Received July 3, 2005

ABSTRACT: The heat capacities, C_p, of poly(oxyethylene), POE, with molar masses from 1500 to 900 000 Da, were analyzed by differential scanning calorimetry (DSC), quasi-isothermal, temperature-modulated DSC (TMDSC), and wide-angle X-ray diffraction (WAXD). There is no change in crystal structure before melting, but the lattice parameters increase rapidly in the melting region. Perfected extended-chain and once- or twice-folded crystals of the oligomers with a molar mass above 1100 Da melt practically fully irreversibly and permit direct measurement of the thermodynamic C_p. The folded-chain crystals of high molar mass show some locally reversible melting. The reversing, apparent C_p depends on molar mass and amplitude and frequency of modulation. After separation from the latent heat effects, the reversible, thermodynamic C_p depends on the melting temperature for low molar masses and increases beyond the vibrational C_p due to conformational motion. Molar masses of 8000−20 000 have almost the same C_p. These observations permit a quantitative discussion of the thermodynamic C_p and the locally reversible melting of the globally metastable POE in the melting range. The increase in C_p between 250 K and the melting temperature is interpreted as a glass transition within the crystal.

Introduction

Thermal analysis, as carried out by standard differential scanning calorimetry (DSC), can produce quantitative heat capacities at constant pressure, p, abbreviated as C_p. The thermodynamic C_p at constant composition, n, is a function of state and is, as usual, defined as

$$C_p = \left(\frac{\partial H}{\partial T}\right)_{p,n} \tag{1}$$

with H representing the enthalpy and T the temperature.[1] For macromolecules, eq 1 for the solid state from 0 K up to the beginning of the glass or melting transition has been quantitatively related to the vibrational motion of the constituent atoms.[1,2] The theory of the thermodynamic C_p(vibrational) is well-enough known to allow extrapolation to higher temperatures, so that the increase of C_p observed at higher temperature can be related to increasing contributions from large-amplitude conformational motion with its accompanying external contribution, largely represented by the difference between C_p and the heat capacity at constant volume, C_v.[1,3]

For semicrystalline polymers, an increasing latent heat effect, $L = (\partial H/\partial n)_{p,T}$, is observed as one approaches the melting transition. The latent heat is either positive (endothermic), as in melting, or negative (exothermic), as in crystallization, annealing, crystal perfection, or recrystallization. The two contributions to H from C_p and L are related to the change in enthalpy:

$$\mathrm{d}H = \left(\frac{\partial H}{\partial T}\right)_{p,n} \mathrm{d}T + \left(\frac{\partial H}{\partial n}\right)_{p,T} \mathrm{d}n \tag{2}$$

where dn indicates the change in composition. For crystallization and melting, for example, n can be replaced by the crystallinity, w_c, with $L = \Delta H_f$ (representing the heat of fusion). Since with scanning calorimetry the change in n cannot be fully controlled, one usually measures an apparent heat capacity $C_p^{\#}$ and the latent heat is computed after subtracting the appropriate C_p from $C_p^{\#}$.[1]

Many of the processes coupled to a latent heat in macromolecules are irreversible. In the past 10 years, commercial temperature-modulated differential scanning calorimetry (TMDSC) has become available for the study of reversibility. The TMDSC can separate irreversible from reversible effects, and a larger number of macromolecules have been studied in this fashion.[4] The response in heat-flow rate, Φ, to the temperature modulation is separated from the response to the underlying effect of scanning with linearly increasing or decreasing temperature by subtracting the sliding average over one modulation period, $\langle\Phi(t)\rangle$, from the instantaneous heat flow rate, $\Phi(t)$. This deconvolution leads to the total heat flow rate, which is similar to the standard DSC result, and to a pseudo-isothermal value from the modulation effect, the reversing heat flow rate.[5] The term reversing is customarily used in the field of TMDSC for the raw data, to distinguish these from the, within the instrumental limits, thermodynamically reversible data. Without further analysis, the recorded reversing heat flow rate may have erroneous contributions when the response to the modulation is nonlinear or the sliding average is nonstationary.[1,4]

Outside the transition ranges, the heat flow rates from the standard DSC and the reversing heat flow rates from TMDSC, given by eqs 3 and 4, respectively, lead usually to identical values of C_p, an indication of full reversibility of the molecular motion:

$$mc_p = \frac{\Delta T}{q}\left[K + C_s \frac{\mathrm{d}\Delta T}{K\,\mathrm{d}T_s}\right] \tag{3}$$

[†] The University of Tennessee.
[‡] Oak Ridge National Lab.

10.1021/ma050861y CCC: $30.25
Published on Web 09/10/2005

$$mc_p = \frac{A_\Phi}{A_{T_S}\omega}\sqrt{1+\tau^2\omega^2} \qquad (4)$$

where m is the sample mass, c_p the specific heat capacity in J K^{-1} g^{-1}, ΔT the temperature difference $T_r - T_s$, a quantity proportional to Φ, with r and s designating reference and sample; q is the heating rate dT_s/dt and A the respective modulation amplitudes. Note that $A_{T_s}\omega$ is the amplitude of the heating rate for a sinusoidal modulation with frequency ω ($= 2\pi/p$, where p is the period in s). If the modulation amplitude is not sinusoidal, a Fourier transformation into the various harmonics is made, and eq 4 applies then to the chosen harmonic (usually the first). The equivalence of q and $A_{T_s}\omega$ demonstrates the similarity of eqs 3 and 4. The second terms in eqs 3 and 4 account for the different dependence of c_p on temperature of reference and sample calorimeters and the different measuring frequencies, respectively. The values of the calibration constants K and τ are usually evaluated empirically by separate runs with sapphire.[1,4]

Within the transition range, the pseudo-isothermal deconvolution of TMDSC data can frequently only yield qualitative results because of instrument lag and loss of stationarity due to the overwhelming amount of latent heat relative to the heat capacity effect and due to slow sample response during melting, crystallization, annealing, crystal perfection, or recrystallization. To avoid this problem, TMDSC without an underlying heating rate, a so-called quasi-isothermal analysis, was developed.[5] In this case, modulation is forced about a constant temperature, T_0, and carried out for extended periods of time. One can then wait for the decay of all irreversible processes occurring at T_0 until a new, metastable state is reached. To cover the whole temperature range of interest, the analysis is then continued at a new, higher or lower T_0. Such quasi-isothermal TMDSC is described in this paper for a large number of poly(oxyethylenes) of different molar mass. The main goal was to separate $C_p^{\#}$ into its up to seven reversible, reversing, and irreversible heat capacity and latent heat contributions and to divide the thermodynamic C_p of eq 2 into the contributions from vibrational and large-amplitude motion. A study of the same samples with wide-angle X-ray diffraction was initiated to follow changes in the crystal unit cell.

Five different types of reversing and reversible latent heats could be established from TMDSC studies of a number of macromolecules:[4] Type 1 is fully reversible melting and crystallization in the presence of crystal nuclei. It was seen in paraffins and low-molar-mass fractions of polyethylene,[6] poly(oxyethylene),[7] and poly(oxytetramethlene).[7] It is limited to chain lengths of ≈75 atoms in the backbone of the molecule. In addition, it was suggested that sufficiently short, decoupled segments of the main or side chain of the macromolecule may similarly crystallize.[4]

Type 2 is the reversing melting which involves distributions of oligomers as they are present in low-molar-mass polymers and also in copolymers. Such melting is usually governed by a eutectic phase diagram.[1] The melting peak is broadened considerably, and the reversibility of melting is limited due to longer times needed to establish the changes in concentrations. These changes in concentration are dictated by the phase diagram in a multicomponent, multiphase system when changing the temperature. For poly(oxyethylene), a time-dependent change of the reversing melting was observed in this case. The reversing, apparent heat capacity increased, as diffusion established a fluctuating concentration gradient in the two-phase region.[8,9]

As the molar mass of the distribution of oligomers increases beyond the critical chain length of ≈75 chain atoms,[6] one finds a small amount of type 3 reversing melting for the extended-chain crystals. The type 3 reversing melting decreases with chain length and crystal perfection, first documented for extended-chain crystals of polyethylene.[10] The fusion is now largely irreversible. The small amount of apparent reversing C_p concentrates within the melting peak.

Type 4 reversing melting refers mainly to crystals with a folded-chain macroconformation,[11] and a portion of it may represent a local melting equilibrium at the surface of the metastable polymer crystals.[12] The reversing latent heat decreases with time before reaching reversibility, a behavior, common in chain-folded crystals, involving slow melting, crystallization, annealing, crystal perfection, or recrystallization (in addition to fast decaying instrument lag).

From paraffins to high-molar-mass PE, one always observes an additional type 5 excess reversible heat capacity which is linked to the isolated local *gauche*−*trans* equilibrium. These local equilibria exist in the crystal and glass of PE, starting far below the transition temperatures. They are better considered as part of the heat capacity, but in the past, they have often been discussed as melting phenomena, hence the name type 5 reversible latent heat. For polyethylene, type 5 C_p is of special importance in the thickening of folded-chain crystals through sliding diffusion.[13] In the present paper, it will be shown that an even bigger effect is observed in poly(oxyethylene) (POE). It will be suggested that this effect can be interpreted as the glass transition of POE crystals.

In this paper, POEs with molar masses from 1500 to 900 000 are analyzed, using standard DSC and TMDSC data to represent the thermal properties between the glass and melting transition. This polymer was chosen because of its easy availability of narrow fractions of low molar mass and polymers of high molar mass. The chosen samples should show no type 1 reversible melting, but some reversing effect of type 2. The extended-chain samples show some type 3 reversing melting, while the high-molar-mass samples have some type 4 reversing and reversible melting, analogous to many prior analyzed flexible macromolecules.[4] All POE crystals will be shown to have type 5 reversible heat capacity which will be considered to be due to a glass transition of the crystals, completed just below the beginning of the major melting temperature. To these five reversing and reversible effects contributing to eq 2, one must add the effects of the irreversible latent heat and the thermodynamic C_p(vibrational).

Experimental Section

Materials. The poly(oxyethylene) fractions, named POE4000, POE10K, and POE20K, were purchased from Polymer Laboratories Ltd., while POE8000 came from Fluka and POE1500 from Polyscience, Inc. The polymers named POE200K and POE900K were purchased from Aldrich. The characteristics of all samples are listed in Table 1, together with samples from the literature which were previously analyzed by TMDSC.[7−9,14] The thermal properties are available from the ATHAS Data Bank.[15] The calculated chain length within the crystal[11] and the equilibrium melting temperatures are also listed for the

Table 1. Characteristic Parameters of the Poly(oxyethylene)s[a]

samples	no. of backbone atoms	weight-average molar mass[b]	M_w/M_n	chain length (nm)	equilib T_m (K)
POE1000[c]	68	1000		6.3	
POE1500[d]	102	1500	1.10	9.0	322.3
POE1960[e]	133	1960	1.03	12.0	326.6
POE3060[e]	208	3060	1.03	18.8	331.7
POE4000	279	4100	1.02	25.4	334.0
POE5000[f]	309	4540	1.05	27.3	334.7
POE8000	568	8350	1.03	51.2	337.5
POE10K	770	11310	1.04	69.4	338.3
POE20K	1460	21450	1.03	131.8	339.5
POE35K[f]	2380	35000		219	
POE200K		M_v ca. 200 000			
POE300K[c]		M_v ca. 300 000			
POE900K		M_v ca. 900 000			

[a] Based on molar mass information supplied by the vendors. [b] Molar mass in Da (daltons). [c] Data for this polymer are available in the literature.[14] [d] Extensive additional data on the same sample are available in the literature.[8,9] [e] Data for this polymer are available in the literature.[7] [f] Data for this polymer are available in the literature.[9]

narrow fractions. The equilibrium melting temperature for a high-molar-mass POE is taken to be 342 K.[15c]

DSC Measurements. Measurements of the apparent heat capacity were carried out with a Thermal Analyst 2920 system from TA Instruments, Inc. The calorimeter is of the isoperibol heat flux, twin type, capable of standard and temperature-modulated modes of operation. The temperature measurement and modulation control are by the sample-temperature sensor. A refrigerated cooling system (RCS) was used, which allowed cooling to 220 K. Dry N_2 gas was purged through the DSC cell with a flow rate of 25 mL min^{-1}. The temperature was calibrated in the standard DSC mode, using the onset temperature of the melting transition peak for indium at 429.75 K, and the heat flow rate was precalibrated at a scanning rate of 10 K min^{-1} with the specific heat of fusion of indium[16] of 28.62 J g^{-1}. The melting temperature of indium was also measured in the quasi-isothermal mode with a 0.5 K temperature amplitude after calibration in the standard mode to identify any differences between two modes of measurement. It was found that quasi-isothermal TMDSC experiments after initial standard DSC calibration led to a melting temperature of 428.89 K. To correct the temperatures from the quasi-isothermal measurements, a constant of 0.86 K was added to the average temperatures of the quasi-isothermal measurements, T_0.

In all the experiments, standard aluminum pans of 20 μL with covers were used for the sample and the empty reference. Three runs of (1) sapphire vs empty reference pan, (2) empty pan vs empty reference pan, and (3) sample vs empty reference pan were carried out for the quantitative measurements. A somewhat lighter reference pan was used for all measurements to approximately correct for the asymmetry of the calorimeter.[17] The standard DSC was performed at 10 K min^{-1} from 273 to 403 K with a 10 min isotherm at the beginning and end. A fresh POE sample was used in the first heating run, followed by the cooling, and a second heating run.

The quasi-isothermal TMDSC was carried out using sinusoidal modulation about successive base temperatures, T_0, with a modulation period of $p = 100$ s, a modulation amplitude of $A = 0.5$ K (unless otherwise stated), and stepwise temperature changes in T_0 of 1−10 K, depending on the changes anticipated in the sample response. The last 10 min of the 20 min quasi-isothermal runs were used for data collection to calculate the reversing C_p from eq 4. Both amplitudes A_Φ and A_{T_s} were calculated as the first harmonics of the Fourier series describing the heat flow rate and the sample temperature, respectively. A standard DSC trace from 253 to 373 K at 10 K min^{-1} was run immediately after the completion of a second cooling run by quasi-isothermal TMDSC to measure the crystallinity of the sample that was annealed during the quasi-isothermal TMDSC steps. Unless otherwise stated, the crystallinity, w_c, shown in the figures was calculated from eqs 1 and 2, where ΔH is derived from the excess heat capacity $C_p^{\#} - C_p$, integrated over temperature for the melting peak, so that the crystallinity is taken as $w_c = (\Delta H/\Delta H_f)$. The heat of fusion of 100% crystalline POE is 196.6 J g^{-1} at the equilibrium melting temperature of 342 K.[15c] More precise calculations, considering the change of the heat of fusion with temperature, are described in the Results section on crystallinity (eq 5).

WAXD Measurements. The X-ray experiments were performed on a Scintag PAD-X powder diffractometer in reflection geometry using unfiltered Cu Kα radiation ($\lambda = 0.154\ 06$ nm). The diffractometer was equipped with a Peltier-cooled solid-state detector. The polymer samples, with dimensions of ≈1 × 8 × 13 mm^3, were mounted on a resistively heated Ta strip. The temperature was controlled with a W/Rh thermocouple directly tack-welded to the Ta strip heater with an accuracy of ±2 K.

A NIST-certified Si powder was mixed with the POE samples to serve as internal standard. The Si 111 reflection at 28.46° served as 2θ calibration. Data in the range of 2θ = 10−42° were collected as a function of temperature from 303 to 335 K. The diffraction peak positions were identified by deconvolution using Pearson-VII functions, and the unit cell parameters were refined from 11 uniquely identifiable reflections based on the known structure.[18] Relative estimates of the crystallinity were made by deconvoluting the crystalline diffraction peaks from the amorphous background.

Results

Thermal Analysis by DSC and TMDSC. The results of all oligomers and polymers of ethylene oxide listed in Table 1 are given in sequence. Prior literature data are summarized briefly for the subsequent discussion and to show the breadth of the available database. The baselines of the thermodynamic heat capacities of the crystals are derived from the analysis of the vibrational spectrum of POE[15f] as described by the ATHAS Scheme.[2,19,20] The melting data for POE are available in the literature and are summarized in Table 2 for crystals of different fold characteristics, close in molar mass to the discussed samples.[21−23]

POE1000. A limited amount of data for a POE sample of 1000 molar mass generated by TMDSC is available in the literature.[14] Similar to the earlier work on POE1500,[8] the oligomer, when well crystallized, gave no indication of a reversing melting peak, although the thermodynamic heat capacity shows an increase beyond that of the vibrational heat capacity, as will be discussed throughout the paper. On fast crystallization at 50 K min^{-1} remnants of the melting of poor, once-folded crystals were suggested to be visible in the standard DSC trace, and reversing effects become visible at 305−309 K, similar to the results the sample of POE1500. The prior analysis of the effects of time and modulation amplitude on TMDSC of POE1500, however, make it

Table 2. Melting Temperature (T_m) and the Number of Folds (n) of Low Molecular Mass POE[a]

	T_m (K)			
M_w	$n = 0$[b]	$n = 1$	$n = 2$	$n = 3$
1500	322.30			
2000	325.85	E		
3500	333.1	325.4	E	
4000	333.55	329.05	E	
4500	333.8	328.6	E	
6000	336.85	333.45	332.15	E
8000	337.45	335.65	334.15	332.95
10000	338.55	337.15	336.05	334.65
20000	340.1			
35000	340.9			
200000	341.8			
300000	341.9			
900000	342.0			

[a] Data from the literature;[21−23] E: short-lived crystals only, followed by annealing to more extended-chain crystals. [b] The equilibrium melting temperature, $T_m°$, for crystals with fully extended chains. For molar masses of 20 000 and higher, this value is estimated from a discussion of the enthalpy and heat of fusion, presented in Figure VIII.15 of the ref 15c.

likely that much of this reversing effect is due to the slow diffusion of the molecules on eutectic crystallization and melting.[9] The rearrangement of hypothetical once-folded intermediates to full chain extension is probably too fast to be discovered by DSC.

POE1500. Figure 1a shows the standard DSC traces of POE1500. The fresh sample reveals a melting peak at 320.1 K and a crystallinity of 85% in the first heating, while the melt-crystallized sample shows a peak of 320.9 K and a crystallinity of about 80% (second heating of the same sample). In the heating runs after long time annealing on cooling by TMDSC, POE1500 shows its major melting peak at 322.3 K with a shoulder at 317.3 K and a higher crystallinity of 88.7%. In the cooling runs at 10 K min^{-1} from the melt, POE1500 shows several overlapping crystallization peaks. According to Table 1, the equilibrium melting temperature, $T_m°$, of POE with a molar mass of 1500 Da is 322.3 K, and the chain length of the extended-chain crystal is 9.0 nm.

The quasi-isothermal experiments show a small peak in the reversing heat capacity on the first heating in Figure 1b, but no reversing melting peak is seen on the second heating in Figure 1c. The reversing melting peak is much narrower than the melting peak of the standard DSC trace since TMDSC is not broadened by instrument lag beyond the modulation amplitude. Figure 1d is an enlarged plot of the reversing heat capacity. The dotted line is the baseline heat capacity of the liquid amorphous sample, while the solid line is the baseline heat capacity of the vibrational contribution to the heat capacity of the solid sample, as given in the ATHAS Data Bank.[15] The first heating gives a melting peak at 317.1 K as well as a minor peak between 278 and 288 K. The end of melting on heating occurs at 321.1 K. The subsequent quasi-isothermal steps on cooling (filled circles) and second heating (triangles) approach the heat capacity of the melt without indication of a latent heat from reversible crystallization and melting transition. A second cooling run was identical to the first run and is not depicted in Figure 1d. The onset of the crystallization on cooling is at 315.2 K, indicating a supercooling of 5.9 K for the crystallization of POE1500. These measurements duplicate the data reported earlier[8] and have been studied in more detail at varying modulation amplitudes and as a function of time.[9]

POE1960. This sample was part of an earlier study.[7] Again, the results are similar to POE1000 and POE1500. As expected from Table 2, the DSC can probably only identify the extended chain crystals. For slowly cooled samples, practically no reversing melting was seen. In

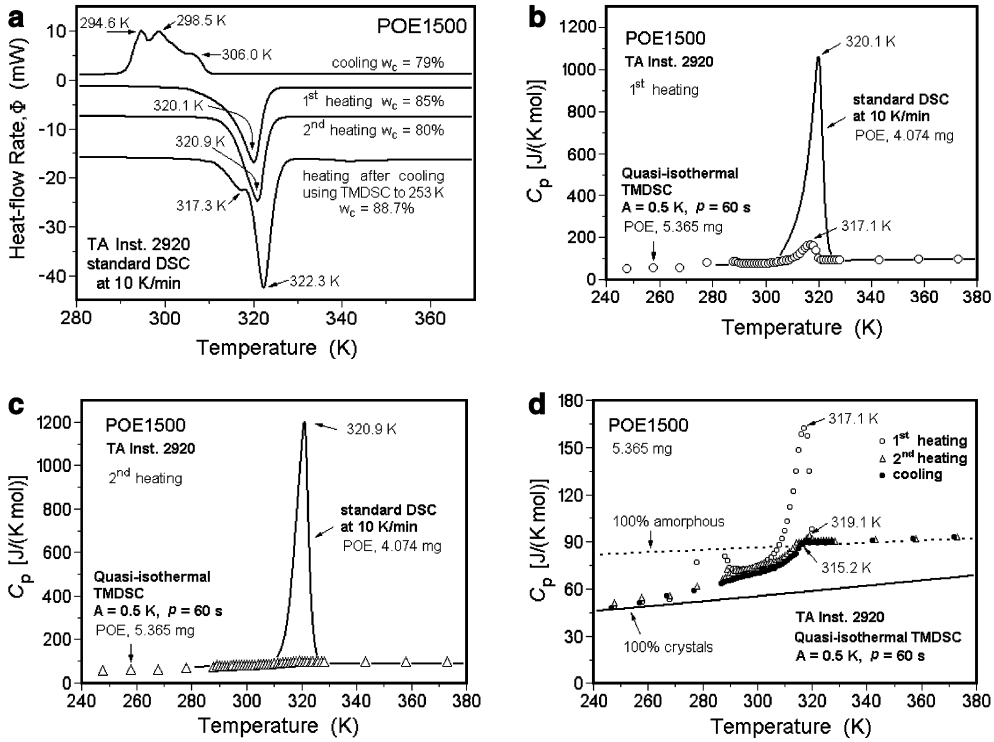

Figure 1. Thermal analysis of POE1500. (a) Standard DSC traces at 10 K min^{-1}. (b) Apparent heat capacities measured by quasi-isothermal TMDSC, first heating of a fresh sample. (c) Apparent heat capacity on second heating of the sample of (b) after a quasi-isothermal run with decreasing T_0 by TMDSC on cooling. (d) Enlarged plots of the TMDSC data on first heating, followed by subsequent cooling, and completed by second heating.

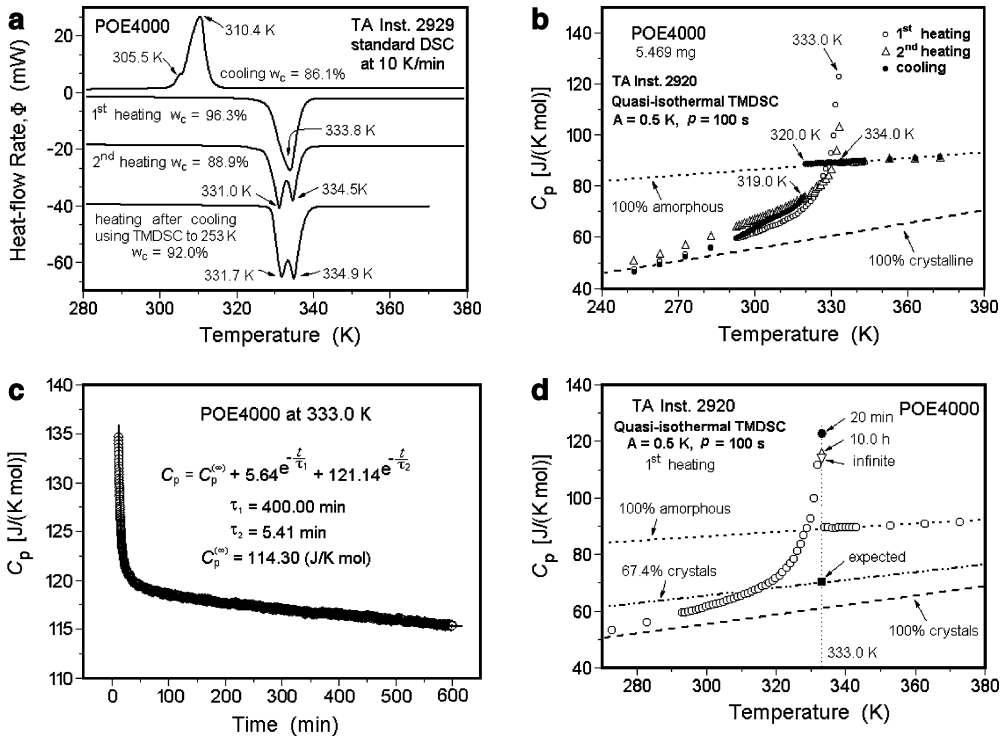

Figure 2. Thermal analysis of POE 4000. (a) Standard DSC traces at 10 K min^{-1}. (b) Apparent heat capacities measured by quasi-isothermal TMDSC on stepwise heating and cooling, enlarged plots for data on first heating, followed by subsequent cooling, and completed by second heating. (c) Time dependence of the apparent reversing heat capacity of the fresh POE4000 in a long-time quasi-isothermal analysis at 333.0 K. (d) Comparison of the apparent reversing heat capacity on long-time, quasi-isothermal analysis at 333.0 K of the fresh POE4000 with the data of the first heating in (b).

the quasi-isothermal TMDSC experiments, the liquid heat capacity was reached at 324.9 K, the expected equilibrium melting temperature of Table 2. A supercooling of 6.6 K made the melting and crystallization fully irreversible.

POE3060. This oligomer was analyzed together with the sample POE1960 and brought a similarly irreversible melting behavior.[7] The standard DSC trace shows both a small melting peak of the once-folded and the main peak of the extended-chain crystals at 325.9 and 331.8 K, respectively, as expected from Table 2. The supercooling for crystallization was 13 K. Again there is only a small reversing peak on TMDSC which decreases further on better crystallization.

POE4000. It can be seen in Figure 2a that the fresh POE4000 shows on standard DSC a melting peak at 333.8 K and a crystallinity of 96.3% in the first heating, corresponding to the extended-chain crystals only (see Table 2). The melt-crystallized sample shows a major peak at 331.0 K and a smaller one at 334.5 K and a crystallinity of about 88.9% (second heating). In the heating runs with a long-time annealing by TMDSC, POE4000 retains these two peaks, but the crystallinity increased to 92.0%. In the cooling runs, POE4000 shows its major crystallization peak at 310.4 K and a shoulder at 305.5 K and reaches a crystallinity of 86.1%.

The details of the quasi-isothermal TMDSC are displayed in Figure 2b. The dotted line is the baseline heat capacity of the 100% amorphous sample, while the dashed line is the vibrational heat capacity for 100% crystalline POE without latent heat contributions, as given in the ATHAS Data Bank.[15] The second cooling run is identical to the first run and not depicted in Figure 2b. A small peak appears in both the first and second trace at 333.0 K, but with a larger contribution on the first heating. The end of the heating is 334.0 K, and the onset of the crystallization on cooling is at 320.0 K. The difference of 14 K represents the supercooling. These results are similar to the POE3060; the reversing peak height is only little higher for both the first and second heating: 123 and 102 J K^{-1} mol^{-1} for POE 4000 compared to 101 and 92 J K^{-1} mol^{-1} for POE3060.

A continuing decrease in the apparent heat capacity was observed near the peak temperature and is shown in Figure 2c with a long-time modulation experiment. A double-exponential fit of the data indicates an ultimately constant level of reversing heat capacity, as summarized in Figure 2d. This constant level of the reversible heat capacity at 333.0 K is still much higher than the expected value for the remaining 67.4% crystallinity at this time and temperature and is also considerably higher than is known for the liquid sample and found for the second heating in Figure 2b.

POE5000. This molar mass was analyzed first as an example of an oligomer which reaches full chain extension.[8] On standard DSC after slow crystallization, it also showed the major melting peak at 331.9 K, close to the $T_m°$ of the extended-chain crystal, and a very small peak at 327.4 K, not far from the once-folded melting temperature. Almost no reversing melting peak was observed on second heating. The supercooling reached about 20 K. As all the other examples analyzed, however, the apparent heat capacity still approaches that of the liquid much faster than expected from the loss of crystallinity.

POE8000. Figure 3a illustrates that in the standard DSC traces there are changes in the behavior of POE8000 relative to the prior samples. The fresh POE8000 shows a single melting peak at 336.1 K at a high crystallinity of 99.5%, with a shoulder on the high-temperature side of the peak. This indicates, based on Table 2, that the sample has a majority of once-folded

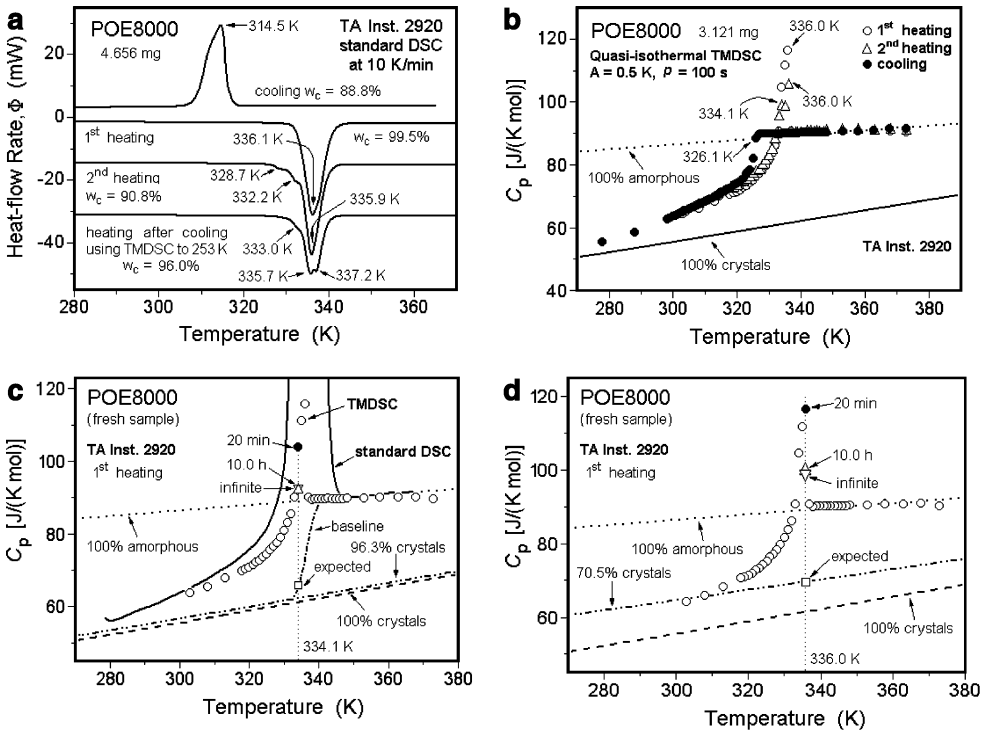

Figure 3. Thermal analysis of POE 8000. (a) Standard DSC traces at 10 K min^{-1}. (b) Apparent heat capacities measured by quasi-isothermal TMDSC on stepwise heating and cooling, enlarged plots for data on first heating, followed by subsequent cooling, and completed by second heating. (c) Time dependence of the apparent reversing heat capacity of the fresh POE8000 in a long-time quasi-isothermal analysis at 334.1 K. (d) Time dependence of the apparent reversing heat capacity of the fresh POE8000 in a long-time quasi-isothermal analysis at 336.0 K (peak temperature).

crystals with only little extended-chain crystals giving rise to the high-temperature shoulder. After cooling from the melt at 10 K min^{-1}, the melt-crystallized sample reveals on second heating a reduced crystallinity of 90.8%, a major melting peak at 335.9 K, and two small peaks at about 332.2 and 328.7 K. This suggests once-folded crystals with small amounts of crystals with $n = 2$ and 3. In the heating run after a long time, stepwise annealing results from the quasi-isothermal TMDSC on cooling, the POE8000 increases in crystallinity to 96.0%, and the double melting peak at 335.7 and 337.2 K suggests that the sample exists of an about equal number of once-folded and extended-chain crystals with only a minor fraction of $n = 2$. In the cooling run the POE8000 shows a crystallization peak at 314.5 K and a shoulder at 312 K yielding a crystallinity of 88.8%.

The quasi-isothermal TMDSC experiments, depicted in an expanded scale in Figure 3b, have a small peak in reversing heat capacity on first heating and an even smaller reversing melting peak on the second heating. The reversing melting peak gets narrower and is located inside the melting peak of the standard DSC (as is seen from Figure 3c). The data from the first and second heating experiments have melting peaks at 336.0 K, and the end of melting occurs at 337.0 K; however, the reversing heat capacity during the second heating has also a peak reaching above the baseline. The subsequent quasi-isothermal steps on cooling approach the heat capacity of the crystal without any reversible crystallization. The onset of the crystallization on cooling is at 326.1 K, indicating a supercooling of about 11 K for POE8000.

In Figure 3c the reversing heat capacity of a fresh POE8000 sample in first heating is compared to the standard DSC result. Also shown is the decrease of the reversing C_p with time at 334.1 K. The reversing heat capacity extrapolates by the method illustrated in Figure 2c to a value at infinite time which is somewhat higher than that of the melt, but much higher than the expected one from the remaining crystallinity. In the second heating, the POE8000 extrapolates at the same temperature to a reversible apparent C_p which is slightly lower than the value of the melt. Figure 3d shows the results from the same experiment as Figure 3c, except being run at the peak temperature, 336.0 K. The apparent reversing of C_p now extrapolates to a small reversible melting at infinite time.

POE10K. The standard DSC trace on first heating of a fresh sample of POE10K shows a single melting peak at 337.0 K and a shoulder at about 334 K, as illustrated in Figure 4a. The crystallinity was 95.4%. When cooled from the melt at 10 K min^{-1}, crystallization peaks occur at 317.9 and 315.9 K, and a crystallinity of 89.2% is reached. In the second heating run, POE10K reveals a melting peak temperature at 337.2 K at a slightly lower crystallinity of 92.0%, with a weak shoulder at about 330 K. However, in the heating runs after long-time annealing by cooling during quasi-isothermal TMDSC, the POE10K sample gives a higher melting peak temperature at 339.8 K and a distinct shoulder at 338.3 K, at a very high crystallinity of 99.9%.

Figure 4b depicts the enlarged plot of the apparent reversing heat capacity data of the quasi-isothermal TMDSC. Both the first heating and second heating experiments reveal a melting peak at 336.3 K, and the end of melting occurs at 338.3 K, but the reversing heat capacity on second heating decreases markedly in peak area above the baseline. The subsequent quasi-isothermal steps on cooling remain at the heat capacity of the melt until the onset of the crystallization at 328.3 K, indicating a supercooling of about 10 K for POE10K.

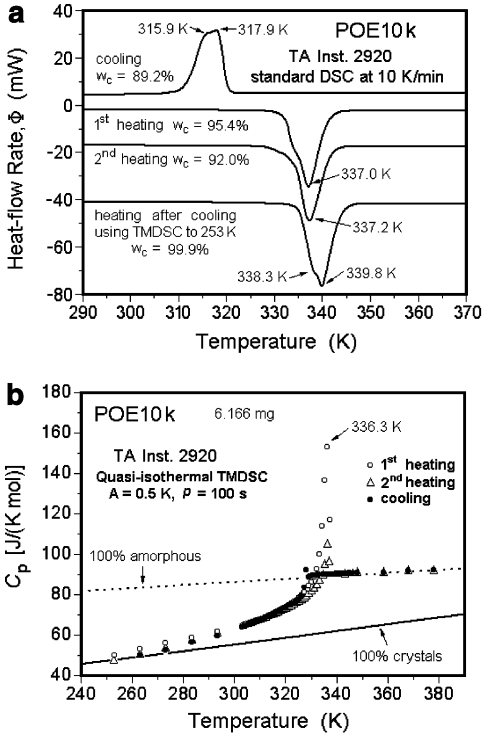

Figure 4. Thermal analysis of POE10K. (a) Standard DSC traces at 10 K min^{-1}. (b) Apparent heat capacities measured by quasi-isothermal TMDSC on stepwise heating and cooling, enlarged plots for data on first heating, followed by subsequent cooling, and completed by second heating.

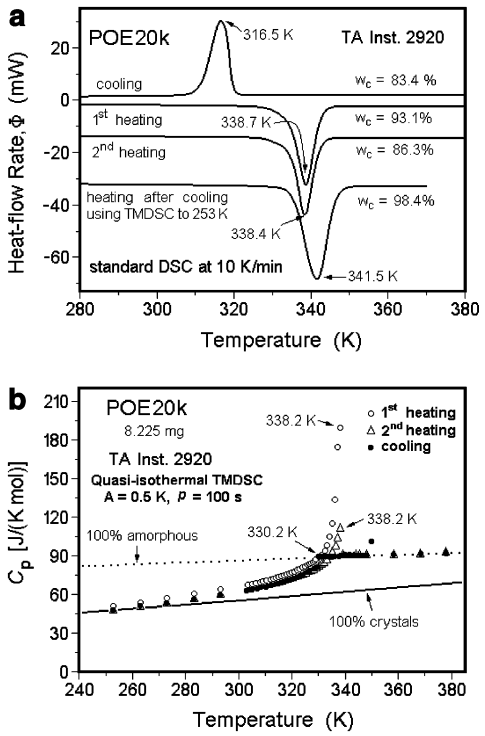

Figure 5. Thermal analysis of POE20K. (a) Standard DSC traces at 10 K min^{-1}. (b) Apparent heat capacities measured by quasi-isothermal TMDSC on stepwise heating and cooling, enlarged plots for data on first heating, followed by subsequent cooling, and completed by second heating.

POE20K. With a molar mass of 20 000 Da, one expects the POE to approach typical polymer properties. Figure 5a represents the standard DSC of POE20K. The fresh sample has a melting peak at 338.7 K and a crystallinity of 93.1%. On second heating, the melt-crystallized sample gives a similar melting peak at 338.4 K, at a crystallinity of 86.3%. In the heating run with a long time annealing by TMDSC, the melting peak shifts to a higher temperature of 341.5 K and yields a crystallinity of 98.4%. In the cooling run, the crystallization peak is at 316.5 K with a crystallinity of 83.4%.

Figure 5b shows the enlarged plot of the reversing heat capacity on quasi-isothermal TMDSC. Both, the first and second heating reveal melting peaks at 338.2 K, and the end of melting on heating occurs at 339.2 K. The reversing heat capacity in second heating decreases in peak area. The subsequent quasi-isothermal steps on cooling approach shows the onset of crystallization on cooling at 330.2 K, indicating a supercooling of about 9 K for POE20K. Long-term quasi-isothermal measurements resulted on first heating at 338.2 K in an apparent reversible C_p of 128 J K^{-1} mol^{-1}, a much higher value than seen for POE8000 in Figure 3d.

POE35K. The properties of POE35K were analyzed earlier.[8] The standard DSC peak occurred at 336.8 K, at the melting temperature of molecules with four folds and the quasi-isothermal TMDSC peak at 337.8, both below the equilibrium melting temperature. The maximum of the reversing heat capacity is 140 J K^{-1} mol^{-1}.

POE200K. The last two samples analyzed with molar masses of 200 000 and 900 000 Da are considered to be of high and very high molar mass, respectively. Figure 6a shows the standard DSC traces of POE200K. The fresh sample reveals a melting peak at 341.0 K and a crystallinity of 94.2% in the first heating, somewhat below the equilibrium melting temperature of 341.8 K listed in Table 2. The melt-crystallized sample gives a lower melting peak at 336.7 K, at a crystallinity of only 70.4%. On heating after a long time annealing by quasi-isothermal TMDSC on cooling, the melting peak also appears at a lower temperature of 337.2 K, but with a crystallinity of 84.4%. In the cooling run from the melt, the crystallization peak occurs at 316.3 K resulting in a crystallinity of 66.1%.

The quasi-isothermal TMDSC experiments in Figure 6b show on the first heating a much higher apparent reversing C_p, but it is still small compared to the standard DSC. Figure 6c illustrates the decrease in the apparent reversing C_p, with the better crystallized sample on second heating. The end of melting is below the equilibrium melting temperature at 340.1 K. Figure 6d represents the expanded plot of the three quasi-isothermal TMDSC series. Different from the lower molar mass POE is that on cooling a small reversing crystallization peak appears at 327.1 K in the quasi-isothermal steps. The onset of the crystallization on cooling is at 329.1 K, indicating a supercooling of about 11 K for POE200K.

POE300K. A sample of this molar mass saw a brief analysis earlier.[14] After slow cooling from the melt, the quasi-isothermal, reversing melting had a maximum of 120 J K^{-1} mol^{-1}, which reduced to 109 J K^{-1} mol^{-1} on slow cooling and a melt end of 335 K. These data should be compared to the ones shown for POE200K.

POE900K. Figure 7a shows the standard DSC results for POE900K. The fresh sample reveals a melting peak at 342.2 K, close to the equilibrium melting temperature listed in Table 2 and the crystallinity is 90.3%. On the second heating, the melt-crystallized sample gives a lower melting peak at 338.4 K with a crystallinity of only 67.1%. In the heating run after long-time annealing by TMDSC, the melting peak appears at 340.0 K, with

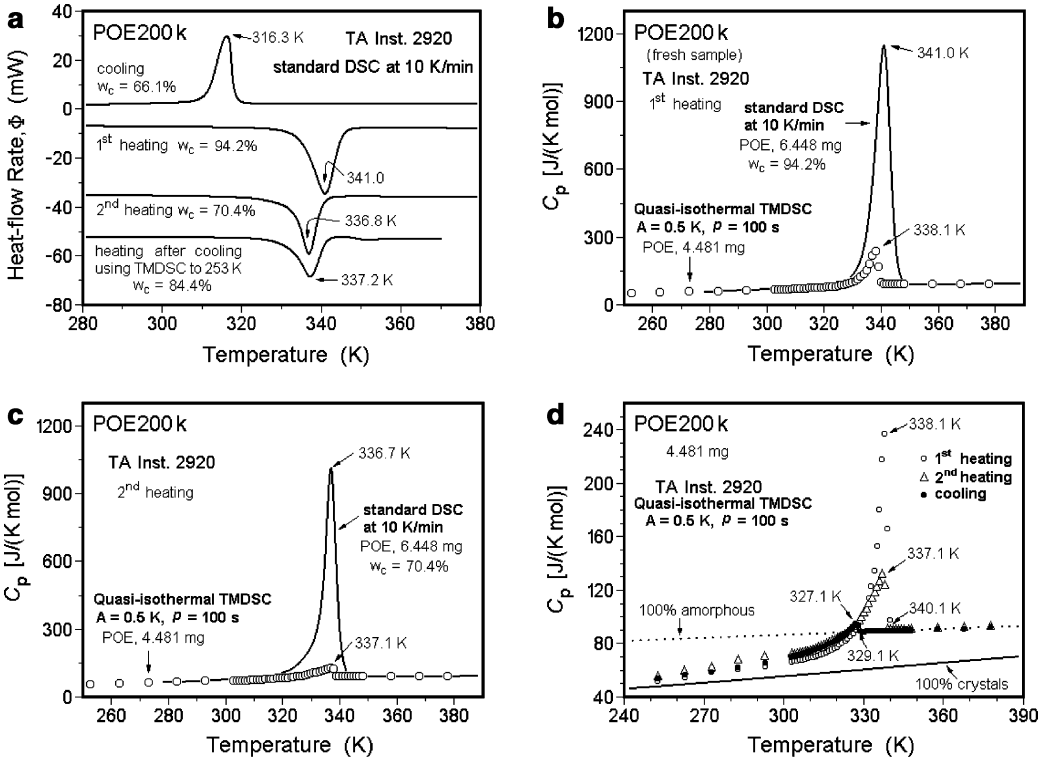

Figure 6. Thermal analysis of POE200K. (a) Standard DSC traces at 10 K min^{-1}. (b) Apparent heat capacities measured by quasi-isothermal TMDSC, first heating of a fresh sample. (c) Apparent heat capacity on second heating of the sample of (b) after a quasi-isothermal run with decreasing T_0 by TMDSC on cooling. (d) Enlarged plots of the TMDSC data on first heating, followed by subsequent cooling, and completed by second heating.

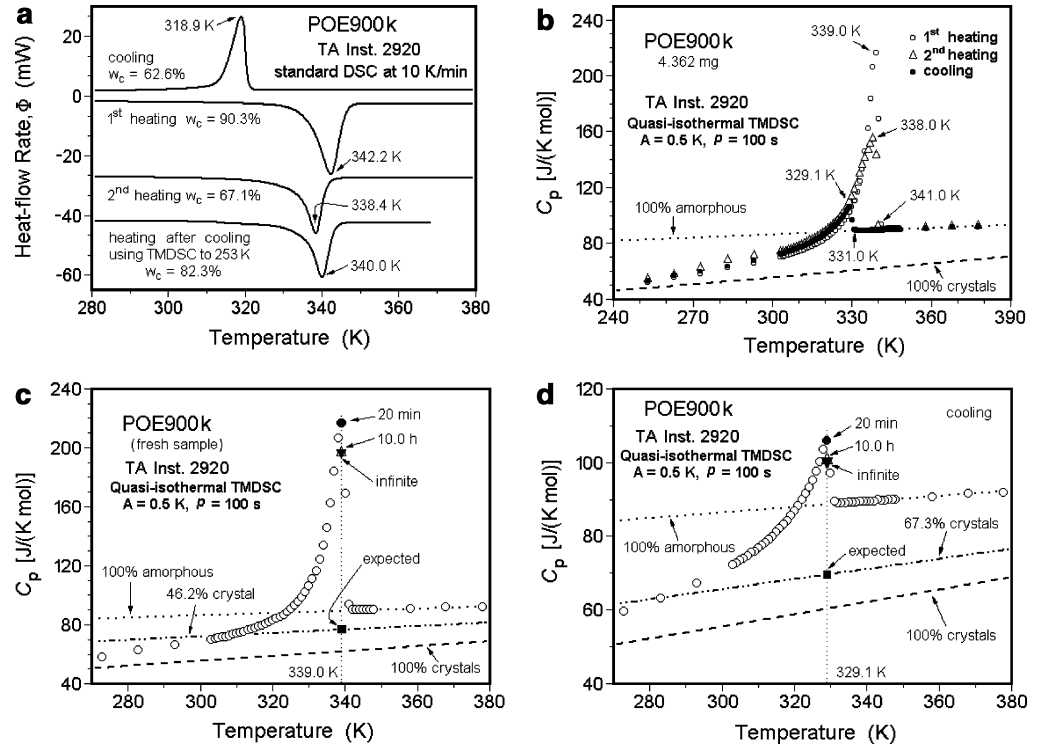

Figure 7. Thermal analysis of POE900K. (a) Standard DSC traces at 10 K min^{-1}. (b) Enlarged plots of the TMDSC data on first heating, followed by subsequent cooling, and completed by second heating. (c) Time dependence of the apparent reversing heat capacity of the fresh POE900K in a long-time quasi-isothermal analysis at 339.0 K (peak temperature). (d) Time dependence of the apparent reversing heat capacity of POE900K in a long-time quasi-isothermal analysis at 329.1 K (peak temperature).

a crystallinity of 82.3%. In the cooling run from the melt, a crystallization peak at 318.9 K with a crystallinity of 62.6% is observed.

The apparent reversing C_p of POE900K from quasi-isothermal TMDSC in Figure 7b gives a similar result to those of POE200K and POE300K. The first heating shows a melting peak at 339.0 K, while the second heating at 338.0 K, and the end of melting on heating occurs at 341.0 K. In the subsequent quasi-isothermal steps on cooling, a reversing crystallization peak ap-

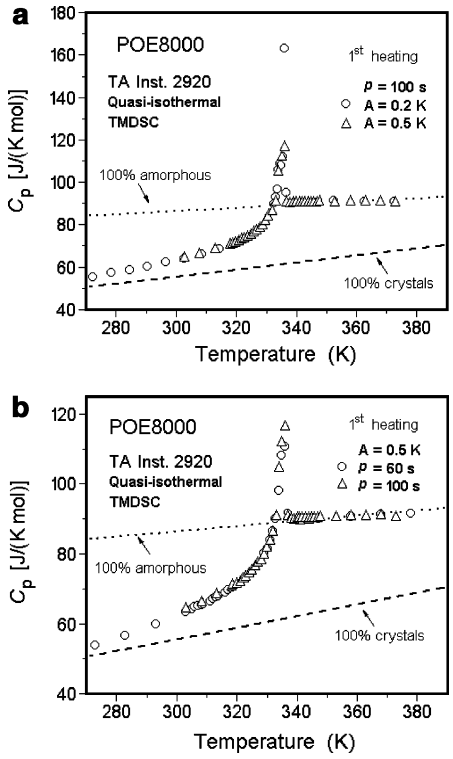

Figure 8. Amplitude, frequency, and molar mass dependence of the apparent reversing heat capacity of POE8000 on quasi-isothermal TMDSC. (a) Changes on first heating for fresh samples when decreasing the modulation amplitude from 0.5 to 0.2 K. (b) Changes in the first heating for fresh samples when decreasing the modulation period from 100 to 60 s.

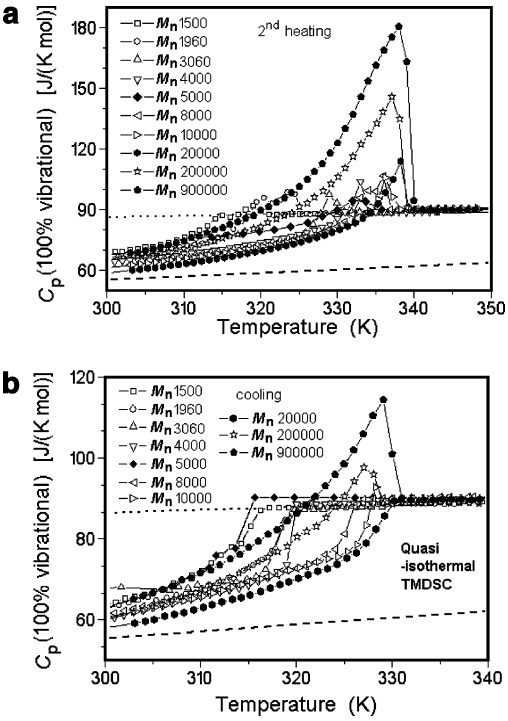

Figure 9. Comparison of the apparent reversing heat capacities measured quasi-isothermally for the crystalline fraction of samples with different molar mass. (a) Changes with molar mass for the second heating experiments. (b) Changes with molar mass for the cooling experiments.

pears at 329.1 K, and the onset of the crystallization on cooling is at 331.0 K, indicating a supercooling of about 10 K for POE900K. Figures 7c contains a comparison of the reversing C_p at various times at 339.0 K for the first heating. Quite clearly, with time the peak values reduce to somewhat smaller reversible values but remain considerably above the heat capacity of the melt of 89 J K^{-1} mol^{-1}; i.e., it must have a reversible melting contribution. Repeating the same experiments at 338 K on second heating reduces the 20 min apparent reversing C_p of about 155 J K^{-1} mol^{-1} to a reversible, apparent C_p of 135 J K^{-1} mol^{-1}. On cooling to successively lower quasi-isothermal temperatures, a clearly measurable reversing melting peak arises at 329.1 K, as is shown in Figure 7d. On long-term experiments it reduces to values still above the C_p of the melt.

Effects of Modulation Amplitude and Frequency. On selected samples the effect of modulation amplitude and frequency was measured. Figure 8a illustrates the effect of the decrease of the modulation amplitude for the POE8000. Decreasing the amplitude from ±0.5 to ±0.2 K has no influence on the heat capacity in the temperature regions below and above the sharp melting peak, i.e., below 330 K and above 338 K. In the melting region, a smaller amplitude produces a larger value of the apparent reversing heat capacity, a result already expected from the nonstationarity of the latent heat contribution. Averaging of the narrow peak over a wider modulation amplitude lowers the average in the deconvolution step.

The frequency dependence is illustrated for the same sample in Figure 8b. At lower frequency (i.e., at longer modulation period), the apparent reversing heat capacity in the melting range is somewhat higher. Below and above the melting range, again, there is no effect, as one would expect for a reversible, equilibrium heat capacity. The frequency effect in the melting range has in the past been linked to the slow kinetics of the melting and crystallization processes.[4] Only the heat capacity based on conformational motion outside the glass and melting transition and vibrational motion has a relaxation time of pico- to femtoseconds and is not affected by frequencies available to the presently used calorimetry and even the new superfast calorimetry (up to 10^6 K s^{-1}).[24]

Effects of Molar Mass on the Reversing Heat Capacity of POE. The molar mass has a marked influence on the apparent reversing C_p of POE, as is obvious from a study of Figures 1−7. In Figure 9, a more quantitative comparison of all data is made after correction of the measurements to 100% crystallinity by subtraction of the heat capacity of the amorphous fraction and increasing the crystalline contribution to 100% by dividing by the mass fraction crystallinity. Figure 9a displays the results for the better crystals of the second heating after slow cooling of the quasi-isothermal runs. Figure 9b shows the results gained during the cooling runs. Below room temperature all samples approach the heat capacity expected from the vibrational heat capacity. The excess of heat capacities beyond the vibrational contribution moves with increasing molar mass to higher temperature. This change goes parallel with the increase in the equilibrium melting temperatures listed in Table 2. This increase continues up to a molar mass of about 20 000. On fusion, the heat capacity of the crystal approaches in all cases the heat capacity of the liquid. The higher molar masses do not have the same C_p vs T profile, as expected from the $T_m°$ of Table 2. Instead of remaining close to the C_p for 8000−20 000, a shift to lower temperature is observed in Figure 9a. This change in direction of the excess in

apparent reversing C_p is coupled with the large reversing melting peak which does not reduce to zero at long times, i.e., is evidence of a reversible melting peak. Even on cooling from the melt, below the crystallization temperature the same increase in C_p is seen in Figure 9b due to reversible melting.

The low-temperature behavior has been analyzed in detail before, using the example of POE1500.[9] The time-dependent changes in the apparent reversing C_p on the low-temperature side of the melting peak were linked at that time to the need of diffusion in the melt on crystallization and melting to accommodate the changes in eutectic equilibrium of the different fractions on changing of the temperature. No further results have been derived for these time-dependent, small, reversing endotherms which are seen in Figure 1d. Except for these diffusion effects, the oligomers, which are known to form extended-chain crystals or have once- or twice-folded molecules within the crystals, show practically no reversing melting on second heating.

Crystallinity. The change of crystallinity with temperature was calculated using the following two phase model:[25]

$$C_p^{\#}(\text{exp}) = w_c C_p(\text{crystal}) + (1 - w_c) C_p(\text{liquid}) - (\mathrm{d}w_c/\mathrm{d}T)\Delta H_f(T) \quad (5)$$

where $C_p^{\#}$(exp) is the experimental, apparent molar heat capacity in the melting range, i.e., the sum of the thermodynamic heat capacity and latent heat exchanged as given in eq 2, C_p(crystal) is the vibrational heat capacity of POE as calculated from its frequency spectrum,[15f] C_p(liquid) is the melt heat capacity extrapolated from measurements above the melting temperature,[15b] w_c is the temperature-dependent crystallinity, and the temperature-dependent heat of fusion is given by $\Delta H_f(T) = H(\text{melt}) - H(\text{crystal})$. It should be noted that C_p of the crystal and glass are usually identical and often used interchangeably in the literature.[1,2,19,20] The crystallinity calculated with eq 5 is usually somewhat higher than the value calculated with a constant heat of fusion at the melting peak. Typical results for POE8000 are shown in Figure 10a. The filled circles in Figure 10a represent the change of crystallinity with temperature during the cooling run, while the open circles are calculated for the seond heating, both for standard DSC experiments as shown in Figure 3a. On cooling from the melt, POE8000 crystallizes at ca. 318 K with a quick increase in crystallinity until 306 K, and then the crystallinity increases very slowly. During the second heating, the crystallinity decreases slowly until ca. 327 K, then it decreases markedly in the melting region, and at about 342 K all crystals are melted. The melt end, determined by standard DSC, must be corrected for instrument lag with data gained from quasi-isothermal TMDSC, as illustrated in Figure 3b.

The same calculations were repeated for all standard DSC traces shown in Figures 1a−7a and are plotted for the second heating run in Figure 10b. Taking the high-crstallinity, largely extended-chain POE8000 as a reference, it is seen that the lower molar mass POE4000 and POE1500 have increasingly lower and broader melting regions, as expected from Table 2. The cooling of POE1500 gives rise to a slower increase in crystallinity with decreasing temperature, again related to the broader range of melting temperatures of the fractions making up this low-molar-mass sample, which yields

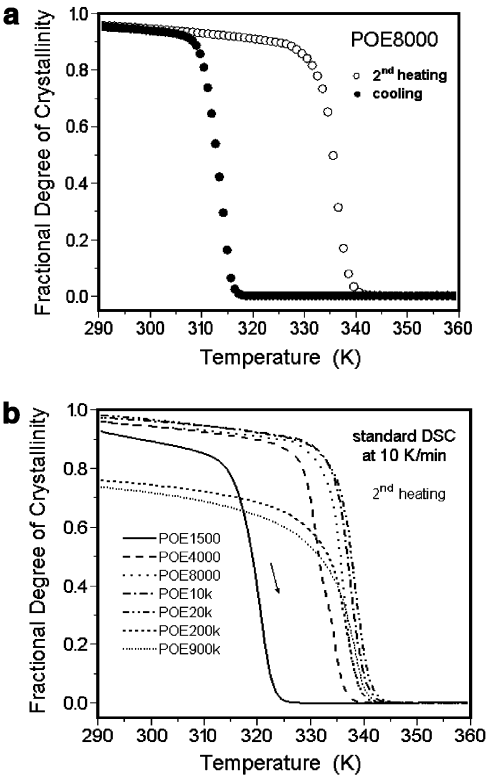

Figure 10. Temperature dependence of the crystallinity of POE of different molar mass, calculated using eq 2. (a) Calculation for cooling and second heating for POE8000 (see Figure 3a). (b) Calculation for the second heating of all samples of POE described in Figures 1a−7a.

the wider crystallization temperature range.[9] For POE10K and POE20K an almost constant behavior is reached, while for the much higher molar masses of POE200K and POE900K, deviations occur due to entanglement and chain folding which leads to broader melting ranges and lower crystallinities. The folded-chain crystals melt over a broader range and reach the end-of-melting at lower temperature due to the reduction in melting temperature by the surface free energy, describable by the Gibbs−Thomson equation for irreversible, zero-entropy production melting.[1]

X-ray Data and Volume of the Unit Cell. To get additional information on the crystals, X-ray data were collected on the POE900K. Figure 11a is a plot of the diffraction pattern, and Figure 11b illustrates the change of the relative dimensions of the unit cell. No changes in the crystal structure were observed up to the complete disappearance of the crystal diffraction. The POE is monoclinic, as described earlier.[26,27]

Figure 11b gives the variation of unit-cell parameters and the volume of the lattice for POE900K. All the unit-cell parameters (a, b, c, and β) increase with temperature, resulting in a two-stage expansion of the crystals volume. A first gradual increase reaches up to 325 K, and the second more rapid increase reaches into the melting region.

Discussion

The discussion is divided into three stages: (1) the standard DSC results, (2) the quasi-isothemal TMDSC data, and (3) the interpretation of the molecular motion derived from the thermodynamic C_p, which consists of the thermodynamic C_p(vibration) and the contribution from conformational motion within the crystal. It should

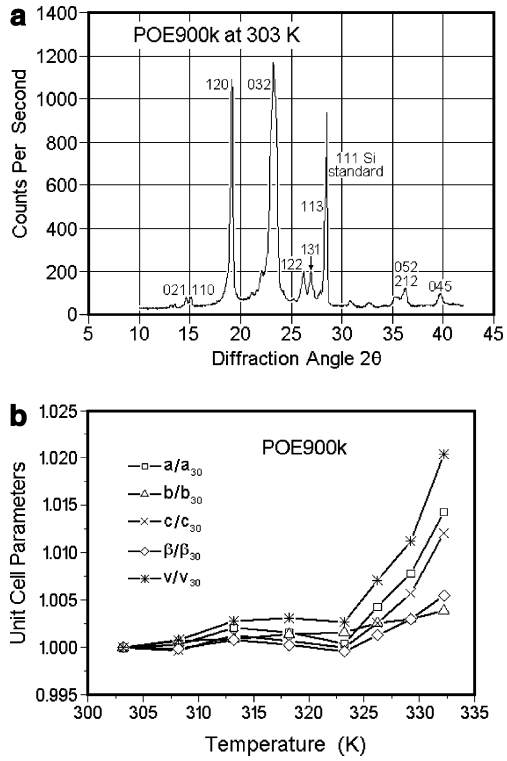

Figure 11. X-ray diffraction data for POE900K, taken as a function of temperature. (a) Diffraction pattern for the monoclinic POE taken at 303 K. (b) Changes of the lattice parameters and the specific volume of the crystals of POE900K as a function of temperature.

be noted also that all throughout the X-ray diffraction data do not allow for a basic change in crystal structure from the pattern shown in Figure 11a. The major change observed is a two-stage increase in unit cell volume, displayed in Figure 11b.

Results of the Standard DSC Experiments. The standard DSC results in Figures 1a−7a reconfirm the earlier connection of melting and crystallization of POE with the extended-chain and folded-chain crystal assignment under the given conditions.[15,21−23] The quantitative changes in crystallinity for the standard DSC on second heating in Figure 10a,b can be consulted for information on the peak area. These data are more precise than the single values listed in Figures 1a−7a, which were calculated with a constant heat of fusion used in eq 5, instead of considering the temperature variation.

The first heating of a sample as delivered by the supplier refers to a POE of unknown crystallization and annealing history, hampering a more detailed discussion. Most samples, however, were powdery and thus most likely crystallized from solution. Commonly, such conditions yield chain-folded crystals of relatively high crystallinity,[28] which in the case of POE anneal quickly. At low molar mass these folded-chain crystals lead to largely extended-chain crystals, as summarized in Table 2 for reference. The empirically found increase of the melting peak with molar mass, following closely the temperatures of equilibrium melting (±1−2 K), results from an accidental cancellation of errors. A sharply melting substance, like indium which is used for the calibration of the DSC, has its equilibrium melting temperature at the extrapolated onset of melting, not the peak. The peak temperature of In is taken as a measure of the instrument lag.[1]

For the crystallization of a low molar mass sample on cooling from the melt under equilibrium conditions, one would expect a gradual crystallization, starting at the liquidus temperature of its phase diagram, completed by a sharp eutectic crystallization peak. The need of crystal nucleation, however, lowers the initial crystallization by 10−25 K when cooling at 10 K min^{-1}. For linear macromolecules, this initial nucleation delay, which would cause a heating to equilibrium at the melting temperature for a sufficiently large sample, is, instead, followed by the further need of molecular nucleation.[28] This molecular nucleation occurs for POE of molar masses exceeding 1000 Da and is in the range of 2−7 K for POE1500−3060.[7] An immediate annealing from folded to more or fully extended-chain crystals further complicate the process at the crystallization temperature and below.[1] In light of this discussion, it is not possible to identify any of the low-temperature crystallization peaks as eutectic peaks. This is borne out by the second heating experiment for POE1500 of Figure 1a, which shows no corresponding eutectic melting peak. The broadness of the crystallization of POE1500 is, thus, only an indication of its substantially larger polydispersity. The possibility of delays of crystallization and melting due to diffusion in the process of approaching equilibrium was discussed before.[9] Nothing will be added to this discussion based on the present DSC and TMDSC results.

After cooling from the melt at 10 K min^{-1}, a repeatable sample has been produced. After the stepwise cooling with 20 min isotherms on quasi-isothermal analysis at successively lower temperatures, the best crystallization is achieved and can be used for a comparison of the samples of different molar mass. Based on Table 2 the following crystal morphologies are suggested to result as a function of molar mass: Below 4000 Da, the crystals were mainly of the extended-chain macroconformation. Both samples of POE4000 and the high-crystallinity samples of POE8000 consist of almost equal mixtures of extended and once-folded crystals. The POE5000 could be crystallized almost fully extended by isothermal crystallization at 320 K.[8] The POE8000 and POE10K samples, cooled at 10 K min^{-1}, are mainly once-folded, with the POE8000 showing distinct, small melting peaks related to crystals with two and three folds per molecule. Following these lower-molar-mass samples of intermediate behavior, POE20K to POE900K, behave like true polymers. The fold lengths vary continuously with crystallization and annealing temperatures.[11] At very high molar mass, the crystallinities decrease (see Figure 10b) and the melting peaks become less reliable due to slow melting and superheating because of interference from entanglements in the amorphous phase. For the further discussion, thus, one can distinguish between the analyses of extended-chain crystals, crystals with a limited number of well-defined folds, and the common crystals of high molar mass with a large number of folds and tie molecules. The first two show only little or no reversible melting, while the last often displays locally reversible melting.[4]

Reversing and Reversible Melting of POE. The changes of the reversing melting with amplitude and frequency for POE8000, as given in Figure 8a,b, follow the expected behavior as detailed in the Results section. The changes with molar mass, in contrast, seem rather involved and will be deconvoluted on the basis of the five types of reversing melting, as summarized in the

Introduction. For a quantitative comparison of the reversing melting in Figures 1−7, Figure 9a,b should be consulted if high-molar-mass samples are involved because of the much lower crystallinity that can arise in these samples. For Figure 9, the apparent reversing heat capacities were recalculated on the basis of 100% crystallinity. The apparent reversing heat capacity is then to be understood as the sum of the thermodynamic C_p(vibrational) and the five types of reversing and reversible latent heat contributions enumerated in the Introduction.[4,29,30]

Type 1, the reversible melting of oligomers below 1000 Da,[7] enters mainly into the description of the low-temperature behavior of POE1000 and POE1500 (Figure 1d). Complication due to irreversible cocrystallization does not allow a further discussion of the type 1 reversible melting. Pure oligomers are needed, as are available for the paraffins, for which this type of reversible melting and crystallization has been discussed fully.[6]

The type 2 reversing melting was described before for POE1500 in more detail.[9] The time effects in quasi-isothermal TMDSC are caused in this case mainly by a temporal decoupling of the phase change and the mixing or demixing of the multicomponent system. For macromolecules, the importance of temporal decoupling of processes and positional decoupling of segments has been discussed recently.[31] The driving force for this partial decoupling in type 2 reversing melting is the need to alter the concentrations of the different species to stay in equilibrium on crystallization or melting to satisfy the changes dictated by the liquidus line of the phase diagram. On quickly changing to the new temperature of modulation, T_0, the time is insufficient to reach the proper concentration of the species melting or crystallizing, and slow adjustment is noted in the reversing melting and recrystallization. In long-time quasi-isothermal experiments the final apparent reversing C_p may reach a steady state of fluctuating concentrations in front of the growing and melting crystals. The typical signature of type 2 reversing melting is its occurrence on the low-temperature side of the melting peak and the increase in amplitude of heat flow rate on long-time quasi-isothermal TMDSC.[9] In the present research, this was observed, as before,[8] for the first melting in Figure 1b,d. On cooling and second melting, the better crystals show practically no reversing melting after the evaluation of the data after 10 min (see also Figure 9a,b). The comparison of standard DSC and TMDSC in Figure 1d reveals a practically fully irreversible melting on the second heating of POE1500.

The type 3 reversing melting is observed in extended-chain crystals of sufficient size to avoid type 1 and 2 reversing melting. It is a small effect and practically disappears on the better crystallization on cooling and on second heating. This has led to the close to fully irreversible melting and crystallization of POE1960 and POE3060,[7] POE4000 (Figure 2b), and POE5000.[8]

As revealed by the standard DSC data, POE8000 on first heating consisted initially of once-folded crystals, which on quasi-isothermal TMDSC would anneal at least partially to extended-chain crystals. Similarly, the mixture of once-folded and extended-chain crystals resulting on slow cooling during quasi-isothermal TMDSC would probably anneal on second heating to a larger fraction of extended-chain crystals. The remaining reversible apparent C_p shown in Figure 3d is thus

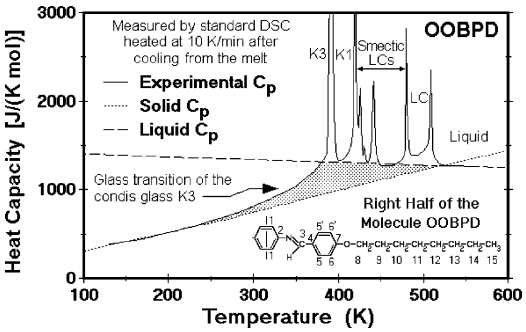

Figure 12. Heat capacity and condis glass transition of the small molecule *N*,*N*′-bis(4-*n*-octylbenzal)-1,4-phenylenediamine (OOBPD).[32]

probably also of type 3. The long-time quasi-isothermal TMDSC at 334.1 K on first heating (Figure 3c) and on second heating (not shown) should both refer to once-folded POE8000. Both experiments suggested a reversible C_p close to that of the liquid. The interesting point of discussion is that these once-folded crystals in POE8000 seem to exhibit no or only little reversible melting, in contrast to the folded chain crystals of high molar mass.

The TMDSC of POE10K and POE20K samples illustrated in Figures 4b and 5b show no reversing melting at the extended-chain melting temperature of Table 2; the standard DSC melting peaks after the TMDSC cooling runs with peak temperatures at the equilibrium, thus, are most likely due to superheating because of slow melting and instrument lag. Figures 4a and 5a are suggesting that the end of melting occurs for the once- or twice-folded crystals. On first heating of POE20K, the reversing peak is much larger than for POE8000, suggesting that now the folded-chain crystals show type 4 reversing melting. The long-term experiments did not reduce the amplitude below that seen on second heating in Figure 5b, i.e., suggest some locally reversible melting.

The reversing melting of POE200K to POE900K, illustrated in Figures 6 and 7, is now clearly of type 4. The reversing melting contribution to the apparent C_p is larger than for type 3, as can be seen best from the comparison in Figure 9a. This revering melting does not decrease significantly at longer times and yields substantial reversible melting (see Figure 7c). Even the crystals growing on cooling show now a sizable reversing and reversible melting, as is best seen in Figures 6d, 7d, and 9b.

Type 5 reversible contributions to the apparent reversing heat capacity should make up the final excess heat capacity. Checking the apparent reversible C_p of quasi-isothermal TMDSC for the samples with no or only little reversing melting in Figure 9a,b, one notices there is always such excess heat capacity which is fully reversible. The beginning of the increase in excess C_p is seen at about 250 K, some 70−90 K below the melting temperatures. This contribution to C_p is dependent on molar mass, but in every case it stops increasing close to the level of the liquid POE, just at the melting temperature, i.e., 20 K lower for the POE1500 than for the POE900K. This increase in C_p behaves like the glass transitions in liquid crystals and condis crystals which cannot form fully ordered crystals on cooling. Figures 12 and 13 give two typical examples of condis crystal glass transitions: one a low-molar-mass material[32] and one a semicrystalline condis crystal.[33] In both cases the

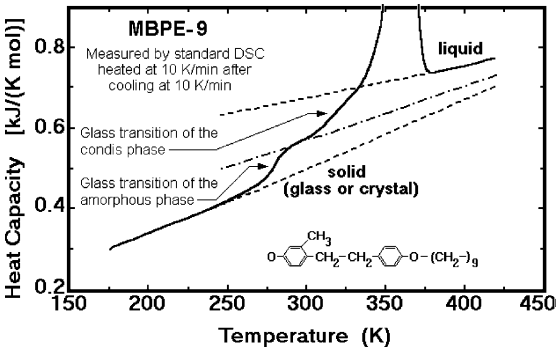

Figure 13. Heat capacity and condis glass transition of the macromolecule poly[oxy(3-methyl-1,4-phenylene)ethylene-1,4-phenyleneoxynonamethylene], MBPE-9.[33]

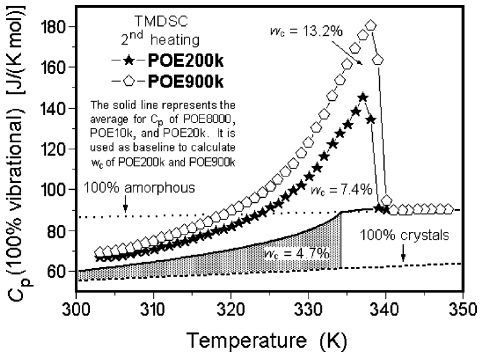

Figure 14. Separation of type 4 apparent reversing and type 5 reversible heat capacities for the samples of POE200K and POE900K on second heating.

glass transition covers a broad temperature region. We assume, thus, a similar glass transition in the crystalline POE and try to justify this assignment in the next section. On this basis, one can separate the type 4 and type 5 contribution on the basis of the data in Figure 9, as is given by the shaded area in Figure 14.

Motion within Crystals of POE. The WAXD results in Figure 11 prove that the POE crystals are monoclinic until melting. The crystal structure of the POE consists of an assembly of 3*7/2 helices which are described approximately by sequences of *trans*−*trans*−*gauche* conformations.[11] On melting, the packing fraction, which is a measure of the occupied volume, decreases by 10% for POE, compared to 14% in polyethylene, but both the melt and the crystal of POE have higher packing fractions (0.65 and 0.72, respectively) than polyethylene (0.60 and 0.70).[15c] The volume of the crystals given in Figure 11b expands with temperature in two stages. Up to about 323 K, the initial expansion starting at low temperature changes into the larger expansion at high temperature. Extrapolating the minor extension to 335 K, one reaches 0.5%, which is close to the crystallinity effect of 4.7% caused by the excess in heat capacity, shown in Figure 14. The sharp expansion beyond 323 K must then be connected with the reversible melting of POE900K and is in urgent need of further research.

The positive deviation from the baseline of the thermodynamic C_p(vibration) given by the ATHAS Data Bank[15] and initially described as type 5 contribution to the reversible heat capacity is most likely connected to conformational motion within the crystals and their accompanying potential energy change. For polyethylene, a similar effect as seen in Figure 14 has been observed, also based on heat capacity analysis. It has

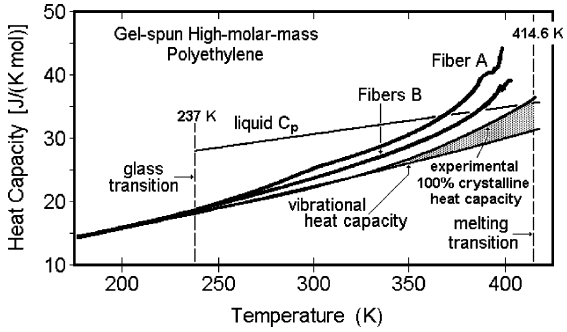

Figure 15. Separation as in Figure 14, but for gel-spun, ultrahigh-molar-mass polyethylene.[34]

served recently to analyze the motion in high-molar-mass, gel-spun polyethylene.[34] Figure 15 illustrates the analysis for two types of these high-strength fibers of different crystallinity. The shaded area corresponds to the conformational contribution which is mainly linked to a local unfreezing of the *trans*−*gauche* equilibrium. The gauche conformations within the orthorhombic crystal of polyethylene and paraffins were proven by IR spectroscopy and molecular dynamics simulation.[13] The same motion is expected to be involved in the glass transition region of the condis crystals of Figures 12 and 13. The nylons with longer sequences of CH_2 groups also show a large, probably reversible, excess heat capacity between the glass transition of the amorphous phase and the melting temperature.[4] In this case quasi-elastic neutron scattering could prove liquidlike motion for the CH_2 groups in nylon-6.6 below the melting temperature.[35] The thermodynamic C_p of crystals of POE consists, thus, of the thermodynamic C_p(vibration) and conformational contributions. The latter freeze in a glass transition between 250 K and the melting temperature.

Conclusions

This extensive study of the thermal properties of POE of different molar masses by DSC, TMDSC, was begun 10 years ago.[7−9] It has clarified the different reversible and reversing contributions to the apparent heat capacity based on the definition of the change in enthalpy of eq 2. Type 1, the reversible melting of small molecules in the presence of crystal nuclei, was analyzed earlier and led to an upper limit of this behavior for small molecules of ca. 75 chain atoms.[7]

Type 2 reversing melting involves a decoupling of the melting and adjustment of concentration for multicomponent oligomers. It was studied earlier in detail on the example of POE1500.[9] In this research these observations were confirmed, but no additional data beyond those of Figures 1 were presented.

Type 3 reversing and reversible latent heat contributions to the apparent heat capacity during melting and crystallization occur mainly in poorly crystallized, extended-chain polymers as shown in Figures 1−3. Such crystals were first analyzed for extended-chain polyethylene.[10] In this research, it was also noted for POE molecules that were only folded once or twice. This type of reversing contribution can be avoided by better crystallization and leads then to fully irreversible melting as seen, for example, in Figure 1c.

Type 4 reversing and reversible latent heat contributions to the apparent heat capacity during melting and crystallization occur mainly in folded-chain polymers of higher molar mass, as seen in Figures 6 and 7, with the transition from lower mass visible in Figures 4 and

5. A full separation from the contribution type 5 is illustrated by Figure 14. This behavior is common to all semicrystalline macromolecules analyzed to date.[4] It has led to the representation of semicrystalline polymers as a global, metastable, nanophase-separated system with locally reversible subsystems.[36] A quantitative treatment of the type 4 effect was proposed earlier for polyethylene.[37]

The main reversible contribution to C_p is the vibrational heat capacity, as was established over the years through ATHAS.[15] To this, the large conformational distribution must now be added as shown as shaded area in Figure 14 (formerly called type 5 reversible contribution to the apparent heat capacity). The excitation of this motion has the behavior of a glass transition within the crystals. Such observation supports the operational definition[38] of a solid as a substance below its glass transition, a definition used over the years by us to teach the subject of thermal analysis of materials.[1] Ordering (with a decrease in entropy) also can lead to a solid state if it causes the freezing of the large-amplitude motion, i.e., a simultaneous glass transition. For rigid, small molecules this is often the case on crystallization. As documented for POE, and discussed above for other examples, the ordering and vitrification may be decoupled, giving rise to new properties to the ordered phase between the ordering and glass transition temperature.

These insights into the thermal properties of flexible macromolecules open many new fields of inquiry concerning the connection of molecular motion to the mechanical properties. The main tools must be, besides DSC and TMDSC, structure analysis, motion analysis, and attempts to model the crystals by molecular dynamics calculations, as has been demonstrated in the past.

Acknowledgment. This work was supported by the Division of Materials Research, National Science Foundation, Polymers Program, Grant DMR-0312233. Use of some of equipment and laboratory space was provided by the Division of Materials Sciences and Engineering, Office of Basic Energy Sciences, U.S. Department of Energy at Oak Ridge National Laboratory, managed and operated by UT-Battelle, LLC, for the U.S. Department of Energy, under Contract DOE-AC05-00OR22725.

References and Notes

(1) Wunderlich, B. *Thermal Analysis of Polymeric Materials*; Springer-Verlag: Berlin, 2005.
(2) Wunderlich, B.; Baur, H. *Fortschr. Hochpolym. Forsch. (Adv. Polym. Sci.)* **1970**, *7*, 151.
(3) Pyda, M.; Wunderlich, B. *Macromolecules* **1999**, *32*, 2044.
(4) Wunderlich, B. *Prog. Polym. Sci.* **2003**, *28*, 383.
(5) Wunderlich, B.; Jin, Y.; Boller, A. *Thermochim. Acta* **1994**, *238*, 277.
(6) Pak, J.; Wunderlich, B. *Macromolecules* **2001**, *34*, 4492.
(7) Pak, J.; Pyda, M.; Wunderlich, B. *Thermochim. Acta* **2003**, *396*, 43.
(8) Ishikiriyama, K.; Wunderlich, B. *Macromolecules* **1997**, *30*, 4126.
(9) Ishikiriyama, K.; Wunderlich, B. *J. Polym. Sci., Part B: Polym. Phys.* **1997**, *35*, 1877.
(10) Pak, J.; Wunderlich, B. *J. Polym. Sci., Part B: Polym. Phys.* **2002**, *40*, 2219.
(11) Wunderlich, B. *Macromolecular Physics;* Academic Press: New York, 1973; Vol. 1.
(12) Okazaki, I.; Wunderlich, B. *Macromolecules* **1997**, *30*, 1758.
(13) Sumpter, B. G.; Noid, D. W.; Liang, G. L.; Wunderlich, B. *Adv. Polym. Sci.* **1994**, *116*, 27.
(14) Albrecht, T.; Strobl, G. *Macromolecules* **1997**, *30*, 7548.
(15) See: (a) ATHAS Data Bank: web.utk.edu/~athas/databank.[1] Specific data for POE for the glass transition by (b) Suzuki, H.; Grebowicz, J.; Wunderlich, B. *Makromol. Chem.* **1985**, *189*, 1109; the melting temperature and heat of fusion on p 66 of (c) Wunderlich, B. *Macromolecular Physics;* Academic Press: New York, 1980; Vol. 3; the heat capacity by (d) Gaur, U.; Wunderlich, B. *J. Phys. Chem. Ref. Data* **1981**, *10*, 1001; and (e) Varma-Nair, M.; Wunderlich, B. *J. Phys. Chem. Ref. Data* **1991**, *20*, 349; the vibrational heat capacity by (f) Grebowicz, J.; Suzuki, H.; Wunderlich, B. *Polymer* **1985**, *26*, 561.
(16) Gmelin, S. M. E.; Höhne, G. W. H.; Cammenga, H. K.; Hemminger, W.; Eysel, W. *Thermochim. Acta* **1994**, *247*, 129.
(17) Ishikiriyama, K.; Wunderlich, B. *J. Therm. Anal.* **1994**, *50*, 337.
(18) Miller, R. L. Crystallographic Data for Various Polymers. In *Polymer Handbook*, 3rd ed.; Brandrup, J., Immergut, E. H., Eds.; Wiley: New York, 1989; p VI/71.
(19) Wunderlich, B. *Pure Appl. Chem.* **1995**, *67*, 1019.
(20) Wunderlich, B. In *Handbook of Thermal Analysis and Calorimetry*; Cheng, S. Z. D., Ed.; Elsevier: Amsterdam, 2002; Vol. 3, p 1.
(21) Buckley, C. P.; Kovacs, A. J. *Prog. Colloid Polym. Sci.* **1975**, *58*, 44.
(22) Buckley, C. P.; Kovacs, A. J. *Colloid Z. Z. Polym.* **1976**, *254*, 695.
(23) Cheng, S. Z. D.; Wunderlich, B. *J. Polym. Sci., Part B: Polym. Phys.* **1986**, *24*, 577.
(24) Wunderlich, B. *J. Therm. Anal. Calorim.*, in press.
(25) Wunderlich, B.; Dole, M. *J. Polym. Sci.* **1957**, *24*, 201.
(26) Tadokoro, H. *J. Polym. Sci., Part C* **1966**, *15*, 1.
(27) Takahashi, Y.; Tadokoro, H. *Macromolecules* **1973**, *6*, 672.
(28) Wunderlich, B. *Macromolecular Physics*; Academic Press: New York, 1976; Vol. 2.
(29) Androsch, R.; Wunderlich, B. *Macromolecules* **1999**, *32*, 7238.
(30) Wunderlich, B. *Thermochim. Acta* **1997**, *300*, 43.
(31) Wunderlich, B. *J. Polym. Sci., Part B: Polym. Phys.* **2004**, *42*, 1275.
(32) Cheng, J.; Jin, Y.; Liang, G.; Wunderlich, B.; Wiedemann, H. G. *Mol. Cryst. Liq. Cryst.* **1992**, *213*, 237.
(33) Jin, Y.; Cheng, J.; Wunderlich, B.; Cheng, S. Z. D.; Yandrasits, M. A. *Polym. Adv. Technol.* **1994**, *5*, 785.
(34) Pak, J.; Wunderlich, B. *Thermochim. Acta* **2004**, *421*, 203.
(35) Xenopoulos, A.; Wunderlich, B.; Narten, A. H. *Macromolecules* **1993**, *26*, 1576.
(36) Wunderlich, B. *Thermochim. Acta* **2003**, *403*, 1.
(37) Androsch, R.; Wunderlich, B. *J. Polym. Sci., Part B: Polym. Phys.* **2003**, *41*, 2157.
(38) Bridgman, P. W. *The Logic of Modern Physics*; MacMillan: New York, 1927.

MA050861Y